

Advanced 2030 Single Aisle Aircraft Modeling for the Electrified Powertrain Flight Demonstration Program

Anusha Harish, Mingxuan Shi, Jonathan Gladin and Dimitri Mavris
School of Aerospace Engineering
Georgia Institute of Technology
Atlanta, Georgia 30332-0250

Emails: aharish9@gatech.edu, mingxuanshi@gatech.edu, jgladin@gatech.edu, dimitri.mavris@aerospace.gatech.edu

Abstract—The NASA Electrified Powertrain Flight Demonstration Program is aimed at advancing electrified powertrains for future aircraft platforms through flight demonstrations for various passenger classes and power levels. The objective of this paper is to establish non-electrified reference models for 2030 aircraft with advanced technologies for the large single aisle (150 passenger) and small single aisle (100 passenger) vehicle classes. Current state-of-art aircraft are first identified and modeled using a proprietary design tool called Environmental Design Space. Next, through a comprehensive literature review, engine, airframe and composite material technologies that are expected to be available by 2030 are identified, and their respective benefits are applied to the 2030 vehicles. The engine cycle and the aircraft design are then optimized to provide the maximum fuel burn benefit while meeting all the specified aircraft requirements. While the large single aisle aircraft range requirement is kept the same as the current state-of-art aircraft, the small single aisle aircraft is optimized for a reduced range of 1000 nmi. Expected fuel burn benefit from these technologies along with any propulsive, aerodynamic and weight benefit will be summarized in this paper.

I. INTRODUCTION

Electrified propulsion aircraft are considered to be a promising solution to meet future environmental goals. Several studies have shown the benefit of these systems for future aircraft. However, there is some uncertainty in the amount of electric drive-train technology development required for these aircraft to be feasible. In order to reasonably estimate the benefit from electrification in the 2030 time frame, it is first necessary to develop advanced 2030 reference non-electrified aircraft models for different vehicle classes. This paper focuses on the development of advanced non-electrified large single aisle (LSA) and small single aisle (SSA) reference aircraft.

II. AIRCRAFT MODELING & SIMULATION ENVIRONMENT

The aircraft models are developed using a multi-disciplinary, physics-based, modeling and simulation environment called Environmental Design Space (EDS) [1], [2]. Primarily developed for assessment of environmental impact of aviation, it consists of a set of tools for performance, noise and emission analyses, integrated using an object-oriented programming language called Numerical Propulsion System Simulation

(NPSS). EDS includes tools such as- Compressor Map Generation (CMPGEN) [3] for off-design axial compressor map generation, NPSS [4], [5] for engine cycle design and analysis, Weight Approximation for Turbine Engines (WATE) [6] for engine flowpath and weight estimation, Flight Optimization System (FLOPS) [7], [8] for aircraft sizing, and Aircraft Noise Prediction Program (ANOPP) [9] for engine and airframe noise analysis. A detailed description of engine and aircraft modeling and analysis using EDS can be found in [2].

III. CURRENT STATE-OF-ART AIRCRAFT MODELS & MISSION REQUIREMENTS

A. Large Single Aisle Aircraft

For the large single aisle vehicle class, the current state-of-art baseline reference model is based on the Airbus A320neo, which is a 150-passenger aircraft with a design range of 6,300 km (3,402 nmi) and maximum cruise speed of Mach 0.82 [10]. With a maximum take-off weight of 79,016 kg (174,200 lb), the aircraft can carry up to 26,725 L (7,060 gallons) of fuel [10]. The aircraft is powered by the Pratt & Whitney geared turbofan engine PW1127G, which weighs about 2,858 kg (6,300 lb) and provides about 120 kN (27,000 lbf) of thrust [12]. The mission profile for the baseline vehicle calibration is depicted in Fig. 1.

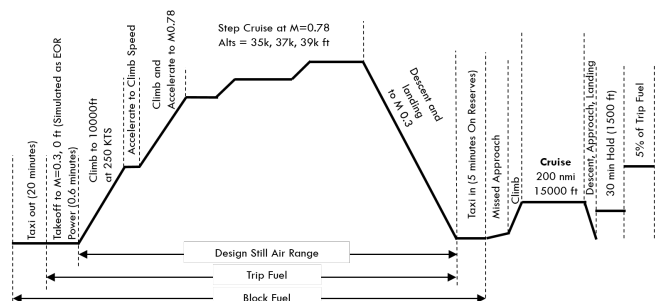


Fig. 1: Notional mission profile for LSA

B. Small Single Aisle Aircraft

For the small single aisle vehicle class, the current state-of-art baseline reference model is based on the Embraer E190-E2, which is a 100-passenger aircraft with a design range of 6,204 km (3,350 nmi) and maximum cruise speed of Mach 0.82 [14]. With a maximum take-off weight of 56,400 kg (124,340 lb), the aircraft can carry up to 16,807 L (4,440 gallons) of fuel [14]. The engines on this aircraft are the Pratt & Whitney geared turbofan engine PW1922G, which weighs about 2,177 kg (4,800 lb) and provides about 106 kN (23,815 lbf) of thrust [13]. Key aircraft specifications for both the aircraft are summarized in Table I.

TABLE I: Baseline Aircraft Key Specifications

	Units	LSA (A320neo [10])	SSA (E190-E2 [14], [15])
Geometry			
Overall length	<i>m (ft)</i>	37.57 (123.25)	36.25 (118.92)
Height	<i>m (ft)</i>	11.76 (38.58)	10.95 (35.92)
Wing span	<i>m (ft)</i>	35.80 (117.42)	33.70 (110.58)
Aircraft Weights			
Max. take-off weight	<i>kg (lb)</i>	79,015.8 (174,200)	56,400 (124,341)
Max. landing weight	<i>kg (lb)</i>	67,403.83 (148,600)	49,050.12 (108,137)
Max. zero fuel weight	<i>kg (lb)</i>	64,319.4 (141,800)	46,700 (102,956)
Max. fuel capacity	<i>L (USgal)</i>	26,725 (7,060)	16,807 (4,440)

IV. ADVANCED 2030 TECHNOLOGIES

The technologies under consideration for the 2030 time-frame are categorized into 3 subgroups - engine, aerodynamics and composite technologies. From a vast set of technologies currently being researched, a subset which are currently at or are predicted to reach Technology Readiness Level (TRL) 9 as defined by the National Aeronautics and Space Administration (NASA) [17] by the year 2030 are selected. A Technology Compatibility Matrix (TCM) is used to identify any incompatibilities and/or interactions between different technologies. The TCM is constructed through one-to-one comparison of each technology to every other technology under consideration and identifying whether they are compatible, incompatible, or any potential interaction. In the TCM, 0's indicate that the two technologies are compatible, 2's indicate that the one of the technologies acts as an enabler for the other, and -1 indicates that the two technologies are incompatible.

The impact of the technologies are then captured through the use of the Technology Impact Matrix (TIM). TIM indicates the impact of each technology on a modelling input variable. In case of incompatible or conflicting technologies, the one with a greater impact on fuel burn reduction is selected.

The technologies incorporated into the advanced 2030 reference vehicles are described in the subsections below.

A. Engine Technologies

Engine technologies are aimed at improving the propulsive efficiency or reducing the engine weight. Technologies such as the advanced powder metallurgy disk [18], advanced

turbine superalloys [19], advanced thermal barrier coatings [20] and Ti-Al turbine stator [21] enable the turbines to withstand higher temperatures without any additional cooling components, improving the propulsive efficiency of the engine. Highly loaded compressor [22] and turbine [23] technologies enable higher stage work while maintaining or increasing the polytropic efficiency of the component. This could lead to a decrease in stage count, therefore decreasing component weight, or an increase in the overall pressure ratio while maintaining the same stage count and without any weight penalty. Composite technologies like the ceramic matrix composites [24] and polymer matrix [25] components lower the engine weight. Advanced nacelle technologies such as the low interference nacelle [26] enable smaller nacelle thickness through improved designs, leading to lower nacelle weight.

B. Aero Technologies

Aero technologies considered are aimed at reducing the aircraft drag. Surface imperfections and excrescences can contribute between 15- 24.5% of aircraft profile drag, representing about 8- 12% of total cruise drag, half of which arise from manufacturing defects [27]–[29]. Excrescence reduction technology can reduce the aircraft profile drag by decreasing the amount of extrusions and surface irregularities through stricter design and manufacturing tolerances. Natural laminar flow control aims to reduce the skin friction drag by delaying the transition from laminar to turbulent airflow over the wing through improved airfoil design. When applied to wing, tails and nacelle, NLF can result in up to 17 % reduction in total airframe drag [30]. Higher aspect ratio (AR) wings can reduce induced drag. However, structural constraints generally limit the maximum allowable AR. With continuous advancement in materials and manufacturing, this AR limit may increase over time [31].

C. Composite Technologies

Composite materials, used on the aircraft wings and tails can significantly help lower airframe structural weight. Pultruded Rod Stitched Efficient Unitized Structure (PRSEUS) is a type of design and fabrication approach that incorporates a one-piece panel with seamless transitions and stitched interfaces, resulting in a lighter and more robust airframe [32], [33]. The composite joints and bolts, grouped together under primary structures joining methodologies, can withstand higher temperature loads, eliminating the need for bulky or heavy joints and thereby, lower the structure weight [35], [36]. Post buckled structures is a design philosophy that allows for structures to fail safely and continue to operate after buckling below their design ultimate load [38], [39]. This reduces the structural weight by allowing structural elements to carry higher loads. Furthermore, fabrication techniques such as Out-of-autoclave, which use a process of vacuum bag forming, act as an enabler for PRSEUS [40], [41].

V. AIRCRAFT DESIGN OPTIMIZATION

Along with incorporation of new technologies, further fuel burn benefits are expected from optimizing the engine cycle

and the aircraft design for 2030. Cycle design optimization is performed by varying the engine cycle parameters such as Fan Pressure Ratio (FPR), Low Pressure Compressor Pressure Ratio (LPCPR), High Pressure Compressor Pressure Ratio (HPCPR), Extraction ratio and maximum burner temperature (T_{4max}). In this study, aircraft design is optimized by varying the thrust-to-weight ratio (T/W), wing loading (W/S), wing sweep angle, wing taper ratio (TR) and wing thickness-to-chord ratio (TCA). A design of experiments is set up by assuming a range of minimum and maximum allowable values for each of these variables, and running several thousands of cases through EDS with different combinations of variable values. The design parameter ranges for the 2030 LSA aircraft are summarized in Table VII. The optimal design is one with minimum fuel burn and meets all performance constraints such as takeoff field length, approach speed, 2nd segment climb with one engine inoperative, etc., (shown in Table III).

TABLE II: Ranges for optimization design parameters

Design parameters	Baseline value	Minimum	Maximum
TWR	0.3093	0.2474	0.3712
WSR	133.09	105.25	157.88
SWEEP	24.41	19.95	29.93
TCA	0.118	0.1	0.15
TR	0.2397	0.2088	0.3132
FPR	1.52	1.35	1.6
OPR	46.9	45	65
HPCPR	13.5	12	19
T_{4max} ($^{\circ}R$)	3380	3000	3600
Ext ratio	1.225	0.9	1.4

TABLE III: Optimization constraints

Constraints	Value
TOFL	< 8000 ft
Vapp	< 140 knots
Wing span	< 118 ft
Core size	> 2.7 lbm/s
Fuel volume	> 10% max fuel weight
OEI 2nd seg climb thrust	> 0

Furthermore, the mission is changed to a cruise climb mission for the LSA aircraft to allow for the vehicle to cruise optimally as shown in Fig. 2.

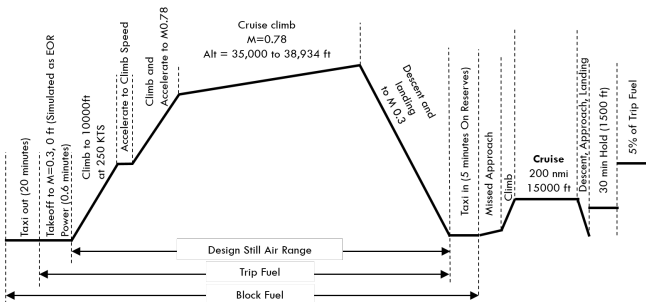


Fig. 2: 2030 LSA Vehicle Notional Mission Profile

For the SSA aircraft, although the typical design ranges may be in the order of 3000 nmi, the range requirement for the advanced 2030 vehicle is reduced to 1000 nmi. Similar design

parameter ranges and performance constraints are assumed for the 2030 SSA aircraft.

VI. RESULTS

A. Current State-of-Art Aircraft

1) *Large Single Aisle Aircraft*: The current state-of-art aircraft based on the Airbus A320neo was calibrated to match the gross weight, maximum takeoff weight, maximum landing weight and maximum zero fuel weight, as specified in [10]. The aircraft engine was calibrated to match PW 1127G specifications such as geometry (fan diameter, nacelle length and diameter, number of compressor and turbine stages, etc.), bypass ratio (BPR), overall pressure ratio (OPR), and weight as shown in Table IV. Thrust, fuel flow and Thrust Specific Fuel Consumption (TSFC) are calibrated to match those in the ICAO databank at sea level static (SLS), takeoff, top-of-climb and cruise as shown in Fig 3.

The chosen design point corresponds to the one with max fuel capacity with nominal payload. The payload range diagram of the EDS model compared to the published diagram in [11] is shown in Fig. 4a. The model is calibrated to match the payload, range, takeoff gross weight (TOGW), operating empty weight (OEW) and fuel burn. The final vehicle performance results are summarized in Table V.

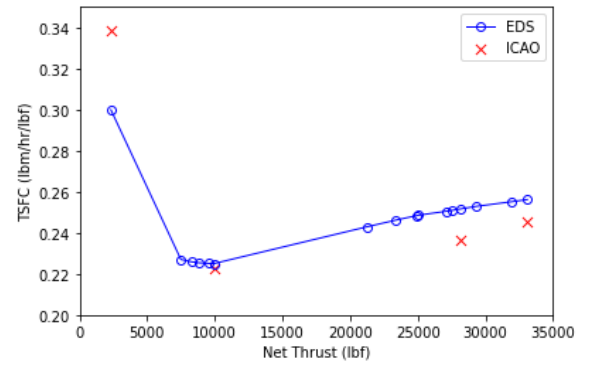


Fig. 3: PW 1127G engine calibration -TSFC vs. Thrust

TABLE IV: Baseline Aircraft Engine Calibration

	Units	PW1133G	GT model
Fan diameter	<i>m</i>	2.06	2.06
	(<i>in</i>)	(81.0)	(81.0)
Dry weight	<i>kg</i>	2,250	2,250
	(<i>lb</i>)	(4,957)	(4,957)
Turbomachinery arrangement	—	1-G-3-8-2-3	1-G-3-8-2-3
BPR (SLS, UI, ISA)	—	11.58	11.58
OPR (SLS, UI, ISA)	—	38.07	38.07
Gear Ratio	—	3	3
Max. nacelle diameter	<i>m</i>	2.55	2.55
	(<i>ft</i>)	8.36	8.36
Max. nacelle length	<i>m</i>	3.51	3.51
	(<i>ft</i>)	(11.51)	(11.51)

2) *Small Single Aisle Aircraft*: Following a similar process as the LSA aircraft, the 100-pax SSA model was calibrated to match the E190-E2 weights, geometry and performance. The results are summarized in Table V. The payload range diagram

of the EDS model compared to the published diagram in the [16] is as shown in Fig. 4b.

TABLE V: Baseline Aircraft Performance

	Units	LSA (A320neo)	SSA (E190-E2)
Design range	km (nmi)	6,300 (3,402)	6,204 (3,350)
Payload @ design range	kg (lb)	15,309 (33,750)	9,580 (21,120)
T/W	(-)	0.3093	0.3817
W/S	kg/m ² (lb/ft ²)	642.33 (131.56)	549.57 (112.56)
TOGW	kg (lb)	79,000 (174,165)	56,400 (124,341)
OEW	kg (lb)	45,068 (99,357)	33,000 (72,752)
Wing area	m ² (ft ²)	123.6 (1,330.5)	103 (1,108.59)
Cruise L/D	(-)	18.229	18.227
SLS thrust	kN (lb _f)	120.42 (27,071)	105.9 (23,814)
SLS BPR	(-)	11.5841	11.1565
Cruise TSFC	kg/N/hr (lb _m /lb _f /hr)	0.0525 (0.5157)	0.0566 (0.5550)
Block fuel @ design range	kg (lb)	16,716 (36,853)	12,452 (27,452)
Block fuel @ economic range	kg (lb)	12,609 (27,797)	8,451 (18,632)

in improved aerodynamic and propulsive efficiencies, weight reduction, and therefore, lower fuel burn for the 2030 aircraft. The major impact of each technology group on the overall aircraft performance is summarized in Table VI.

TABLE VI: Technology impact on aircraft performance

Impact	LSA	SSA
Engine tech: TSFC benefit	-3.00 %	-2.75 %
Aero tech: L/D benefit	+13.35 %	+3.45 %
Composite tech: OEW benefit	-9.07 %	-7.11 %

Results for the LSA advanced 2030 aircraft indicate a total fuel burn benefit from all technologies of about 15.90%. An additional 4.94% benefit can be obtained by optimizing the aircraft design and engine cycle, resulting in a total of 20.05% compared to the 2018 LSA TRA. The results from the optimization process, in terms of the final aircraft design parameters and the constraint diagram with performance constraints is shown in Table VII and Fig. 5 respectively. Finally, by allowing the aircraft to cruise climb, an additional 0.4% fuel burn benefit is expected. The fuel burn benefit from each individual technology group, as well as from the aircraft and mission optimization is shown in Fig. 6.

Results for the SSA advanced 2030 aircraft indicate a total fuel burn benefit of about 12.06%. By reducing the design range from 6,204 km (3,350 nmi) to 1,852 km (1,000 nmi) can provide an additional 6.45% fuel burn benefit. Furthermore, optimizing the engine cycle and the aircraft design can lead to another 4.77%, summing up to 21.10% compared to 2018 SSA TRA. The fuel burn benefit at economic mission range of 1,852 km (1,000 nmi), from each individual technology group, reduced design range, aircraft and engine cycle optimization is shown in Fig. 7.

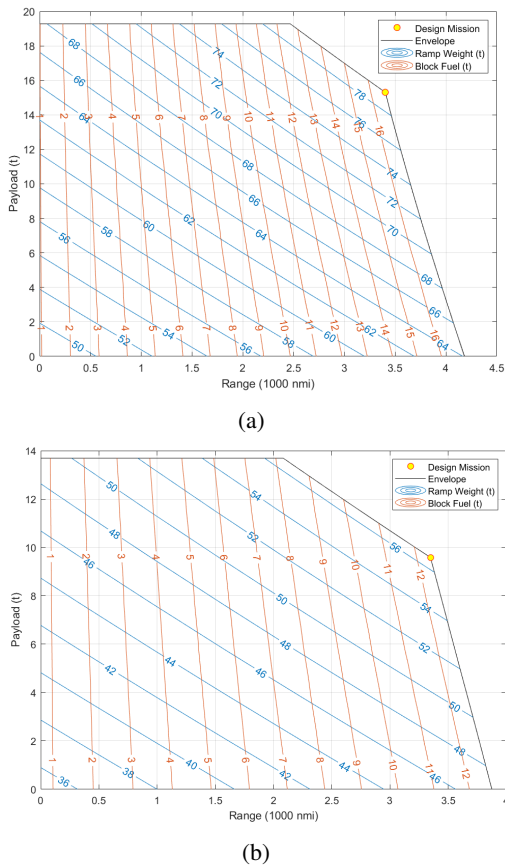


Fig. 4: Payload range diagrams for (a) LSA and (b) SSA

B. Advanced 2030 Non-electrified Aircraft

The technologies described in Section IV are added on to the 2018 Technology Reference Aircraft (TRA) resulting

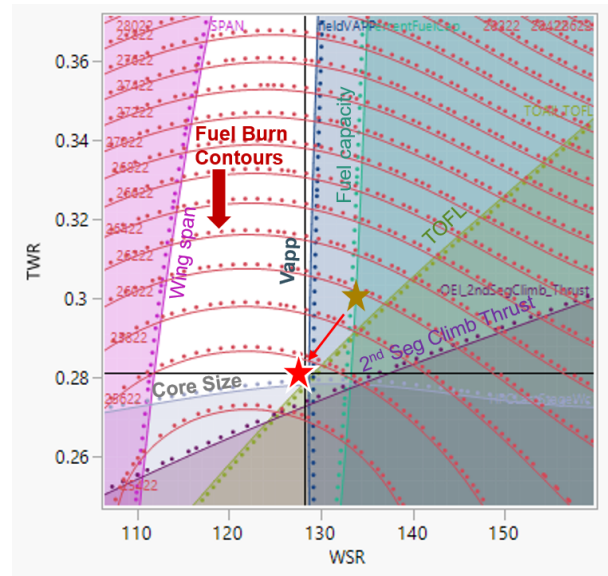


Fig. 5: LSA Constraint diagrams - Thrust-to-weight ratio vs. Wing loading

TABLE VII: Optimized design parameters for 2030 LSA

Design parameter	LSA		SSA	
	2018 TRA	2030 Optimized	2018 TRA	2030 Optimized
TWR	0.3093	0.2811	0.3817	0.3612
WSR	133.09	128.23	101.88	97.14
SWEEP	24.41	21.2	26.24	22
TCA	0.118	0.11	0.096	0.096
TR	0.2397	0.21	0.301	0.26
FPR	1.52	1.36	1.5	1.445
OPR	46.9	53	45.25	46
HPCPR	13.5	18	13.5	17.5
T4max (°R)	3380	3125	3375	3075
Ext ratio	1.225	1.13	1.26	1.3

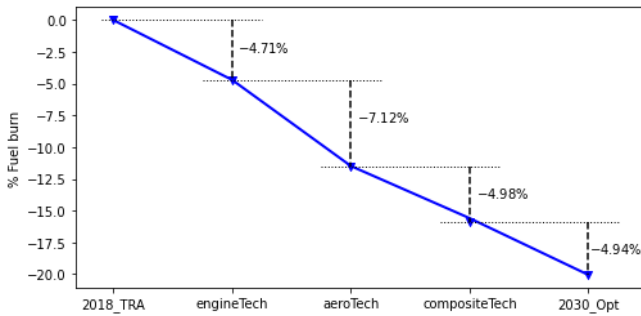


Fig. 6: LSA fuel burn benefit

VII. CONCLUSION

The purpose of this paper is to establish advanced non-electrified reference aircraft models for the Large and Small Single Aisle aircraft classes for the 2030 Entry-into-Service timeframe. To this end, current state-of-art aircraft models were developed based on the Airbus A320-neo and the Embraer E190-E2 for the LSA and SSA classes respectively using the modeling and simulation environment, EDS. Promising engine, aerodynamic and composite material technologies that are at or are projected to reach TRL 9 by 2030 were selected and modeled, improving propulsive or aerodynamic efficiency, or reducing weight. Furthermore, the engine cycle and aircraft design were also be optimized for maximum fuel burn benefit.

The advanced 2030, 150-pax LSA aircraft is expected to have 20.45% fuel burn benefit with advanced technologies, optimized aircraft design, engine cycle and mission. Similarly, the advanced 2030, 100-pax SSA aircraft is expected to have 21.10% fuel burn benefit. These aircraft models will serve as the baseline against which the benefit of electrified propulsion is compared in [43].

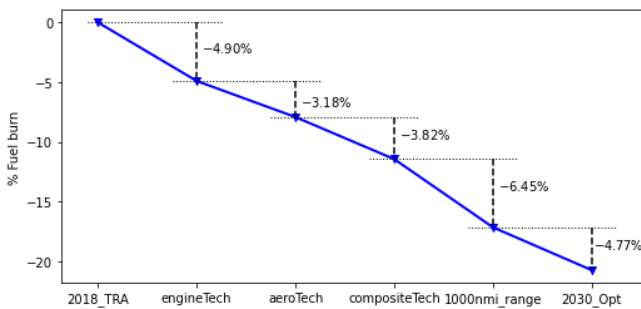


Fig. 7: SSA fuel burn benefit

ACKNOWLEDGMENT

The authors would like to thank NASA for their support of this effort under AWD-002344 (NIA-602015), especially Gaudy Bezos-O'Connor, Ralph Jansen, and Fayette Collier.

REFERENCES

- [1] M. Kirby and D. N. Mavris, "The environmental design space," in *26th Int. Congr. of the Aeronautical Sciences*, Anchorage, AK, 2008.
- [2] L. S. Nunez, J. Tai and D. N. Mavris, "The environmental design space: modeling and performance updates," in *AIAA SciTech Forum*, Virtual Event, 2021.
- [3] *Extended Parametric Representation of Compressors Fans and Turbines. Vol. I- CMPGEN User's Manual*, National Aeronautics & Space Administration, 1984. CR-174645.
- [4] R. Claus, A. Evans, J. Lytle and L. Nichols, "Numerical Propulsion System Simulation," *Computing Systems in Engineering*, vol 2, No. 4, pp. 357-364, 1991.
- [5] J. Lytle, G. Follen, C. Naiman and A. Evans, "Numerical Propulsion System Simulation (NPSS) 1999 industry review," Tech. rep., National Aeronautics & Space Administration, 1999. TM-2000-209795.
- [6] M. Tong, I. Halliwell and L. Ghosn, "A computer code for gas turbine engine weight and disk life estimation," *J. Eng. Gas Turbines Power*, vol. 126, No. 2, 2004, pp. 265-270.
- [7] *Flight Optimization System: release 8.11 user's guide*, National Aeronautics & Space Administration, Oct 2009.
- [8] D. P. Wells, B. L. Horvath and L. A. McCullers, "The Flight Optimization System weights estimation method," Tech. rep., 2017. TM-2017-219627.
- [9] W. Zorunski, "Aircraft Noise Prediction Program Theoretical Manual," Tech. rep. NASA, 1982, TM-1982-83199.
- [10] *A320neo*, Airbus, France, Accessed on: Jul. 20, 2020. [Online]. Available: <https://aircraft.airbus.com/en/aircraft/a320/a320neo>
- [11] *Airbus, AC 320: Aircraft Characteristics Airport and Maintenance Planning*, Airbus, France, Accessed on: Jul. 20, 2020. [Online].
- [12] *Geared Turbofan: PW1100G-JM*, Pratt & Whitney, Jun 2019.
- [13] *Type-certificate Data Sheet No. IM.E.090 for PW1500G Series Engines*, Pratt & Whitney, March 2019.
- [14] *E190-E2*, Embraer, Accessed on Jul. 20, 2020. [Online]. Available: <https://www.embraercommercialaviation.com/commercial-jets/e190-e2-commercial-jet/>
- [15] *Embraer E190-E2 Specifications*, GlobalAir, Accessed on Nov. 17, 2021. [Online]. Available: <https://www.globalair.com/aircraft-for-sale/Specifications?specid=1630/>
- [16] *Embraer, E-Jets E2: Airport Planning Manual*, Embraer, Accessed on Jul. 20, 2020. [Online].
- [17] National Aeronautics and Space Administration, *Technology Readiness Level*, National Aeronautics and Space Administration, Accessed on: Sep. 07, 2020. [Online].
- [18] R. Schafrik and R. Sprague, "Superalloy technology - a perspective on critical innovations for turbine engine," *Key Engineering Materials*, vol. 380, 2008.
- [19] T. M. Pollock and S. Tin, "Nickel-based superalloys for advanced turbine engines: chemistry, microstructure, and properties", *AIAA Journal of Propulsion & Power*, vol. 22, No. 2, 2006.
- [20] D. Zhu, R. A. Miller and D. S. Fox, "Thermal and environmental barrier coating development for advanced propulsion engine systems," in *48th AIAA/ASME/ASCE/AHS/ASC Structures, Structural Dynamics, & Materials Conf.*, Honolulu, HI, 2007. AIAA 2007-2130.
- [21] W. Smarsly, "Aero engine materials," presented at MTU seminar, Cracow University of Technology, Poland.
- [22] T. Dickens and I. Day, "The design of highly loaded axial compressor," *Journal of turbomachinery*, vol. 133, Jul 2011.
- [23] J. T. Schmitz et al. "Highly loaded low pressure turbine: design, numerical, and experimental analysis," in *Proc. of ASME Turbo Expo 2010: Power for land, sea and air*, Glasgow, Scotland, 2010.
- [24] P. L. M. Murthy, D. Brewer and A. R. Shah, "Environmental/ thermal barrier coatings for ceramic matrix composites: thermal tradeoff studies", Tech. rep., National Aeronautics & Space Administration, Jul 2007.
- [25] K. Steffens and H. Wilhelm, "Next engine generation: materials, surface technology, manufacturing processes- what comes after 2000?" presented at MTU Aero Engines, Munchen.

TABLE VIII: LSA Vehicle Results Summary

Vehicle parameters	Units	2018 TRA	2030 Vehicle	% Change w.r.t. 2018 TRA	2030 Optimized	% Change w.r.t. 2018 TRA	2030 Optimized w/ Cruise Climb	% Change w.r.t. 2018 TRA
Block fuel @ design range (6,300 km)	kg (lb)	15,546.1 (34,279.2)	13,073.6 (28,827.3)	-15.90 %	12,427.7 (27,403.1)	-20.06 %	12,366.8 (27,268.7)	-20.45 %
Block fuel @ econ range (921 km)	kg (lb)	2,756.8 (6,078.8)	2,372.2 (5,230.8)	-13.95 %	2,240.6 (4,940.4)	-18.73 %	2,238.9 (4,936.7)	-18.79 %
Cruise SFC	kg/s/kN (lbm/hr/lbf)	0.0148 (0.5229)	0.0144 (0.5093)	-2.60 %	0.0141 (0.4974)	-4.88 %	0.0141 (0.4975)	-4.86 %
TOGW	kg (lb)	76,801.8 (169,348)	72,443.1 (159,737)	-5.68 %	72,130.6 (159,048)	-6.08 %	72,042.6 (158,854)	-6.20 %
OEW	kg (lb)	43,226.8 (95,315.1)	41,556.8 (91,654.9)	-3.84 %	42,162.9 (92,696.3)	-2.46 %	42,139.8 (92,918.3)	-2.51 %
SW	m ² (ft ²)	118.5 (1,275.2)	111.5 (1,200.2)	-5.88 %	115.4 (1,242.6)	-2.56 %	115.3 (1,241.1)	-2.67 %
Sea Level Static BPR	—	11.37	13.14	15.57 %	14.17	24.53 %	14.16	24.54 %
Start of Cruise LoD	—	18.79	21.08	12.18 %	21.58	14.85 %	21.58	14.85 %
Fan diameter	m (in)	1.83 (72.2)	1.79 (70.4)	-2.49 %	1.98 (77.9)	7.89 %	1.98 (77.9)	7.89 %
Nacelle diameter	m (in)	2.34 (92.2)	2.30 (90.4)	-1.95 %	2.49 (97.9)	6.18 %	2.49 (97.9)	6.18 %

TABLE IX: SSA Vehicle Results Summary

Vehicle parameters	Units	2018 TRA	2030 Vehicle	% Change w.r.t. 2018 TRA	2030 Reduced Range	% Change w.r.t. 2018 TRA	2030 Optimized	% Change w.r.t. 2018 TRA
Block fuel @ design range (3350 nmi)	kg (lb)	11,980.5 (26,417)	10,535.7 (23,231.2)	-12.06%	-	-	-	-
Block fuel @ econ range (1000 nmi)	kg (lb)	3,925.2 (8,655.1)	3,476.2 (7,665.0)	-11.44%	3,252.1 (7,170.8)	-17.15 %	3,097.0 (6,828.9)	-21.10 %
Cruise SFC	kg/s/kN (lbm/hr/lbf)	0.0154 (0.5446)	0.0151 (0.5335)	-2.04%	0.0156 (0.5494)	0.88 %	0.0155 (0.5456)	0.18 %
TOGW	kg (lb)	56,390.5 (124,341)	51,754.2 (114,118)	-8.22%	41,643.08 (91,823)	-26.15 %	40,092.5 (88,404)	-28.90 %
OEW	kg (lb)	33,515 (73,900.5)	30,464.4 (67,174.1)	-9.10%	27,698.1 (61,074.3)	-17.36 %	26,377.1 (58,161.6)	-21.30 %
SW	m ² (ft ²)	113.8 (1,224.7)	104.4 (1,124)	-8.22%	84.1 (904.8)	-26.12 %	84.9 (913.6)	-25.4 %
Sea Level Static BPR	—	11.17	13.79	23.46%	13.04	16.74 %	11.97	7.16 %
Start of Cruise LoD	—	19.23	19.75	2.74%	18.95	-1.45 %	19.31	0.41 %
Fan diameter	m (in)	1.85 (73)	1.78 (70.1)	-3.97%	1.59 (62.8)	-13.97 %	1.61 (63.3)	-13.29 %
Nacelle diameter	m (in)	2.21 (86.9)	2.13 (83.9)	-3.45%	1.95 (76.7)	-11.74 %	1.96 (77.2)	-11.16 %

[26] R. E. Owens, K. L. Hasel and D. E. Mapes, "Ultra high bypass turbofan technologies for the twenty-first century," Tech. paper, 1990. AIAA 90-2397.

[27] A. K. Kundu, J. K. Watterson, and S. Raghunathan, "A multi-disciplinary study of aircraft aerodynamic surface smoothness requirements to reduce operating cost," in *7th AIAA/USAF/NASA/ISSMO Symp. on Multidisciplinary Analysis and Optimization*, St. Louis, MO, 1998, AIAA 1998-4874-126.

[28] M. Sanchez, A. K. Kundu, B. K. Hinds and S. Raghunathan, "A methodology for assessing manufacturing cost due to tolerance of aerodynamic surface features on turbofan nacelles," *Int J Adv Manuf Technol*, vol. 14, pp. 894-900, Dec 1998.

[29] A. D. Young and J. H. Paterson, "Aircraft Excrescence Drag," *NATO Advisory Group for Aerospace Research and Development*, Jul 1981.

[30] B. J. Holmes, C. C. Croom, E. C. Hastings, Jr., C. J. Obara and C. P. van Dam, "Flight research on natural laminar flow," in *NASA Langley Symposium on Aerodynamics*, vol 1, pp. 461-474, Dec 1986.

[31] *Commercial aircraft design characteristics - trends and growth projections*, International Industry Working Group, 5th Edition R1, 2007.

[32] D. Jegley and A. Velicki, "Status of advanced stitched unitized composite aircraft structures," in *51st AIAA Aerospace Sciences Meeting*, Grapevine, TX, 2013, AIAA 2013-0410.

[33] A. Velicki and D. Jegley, "PRSEUS Structural Concept Development," in *AIAA Aerospace Sciences Meeting*, National Harbor, MD, 2014, AIAA 2014-0259.

[34] D. Jegley and A. Velicki, "Development of the PRSEUS multi-bay pressure box for a hybrid wing body vehicle," in *56th AIAA/ASCE/AHS/ASC Structures, Structural Dynamics, & Materials Conf.*, Kissimmee, FL, 2015, AIAA 2015-1871.

[35] M. McCarthy, "BOJCAS: bolted joints in composite aircraft structures," *Air & Space Europe* vol. 3, pp. 139-142, 2001.

[36] R. J. Miller, M. E. Palusis and D. C. Jarmon, "Composite fastener for use in high temperature environments," U.S. Patent 6.045.310, United Technologies Corporation, Hartford, CT, Apr 2000.

[37] R. Bossi and M. J. Hiehl, "Bonding primary aircraft structure: the issues," *Manufacturing Engineering*, vol. 14, No. 3, pp 101, Mar 2011.

[38] L. J. Kootte et al., "Effect of composite stiffened panel design on skin-stringer separation in postbuckling," in *AIAA SciTech Forum*, Virtual Event, Jan 2021.

[39] O. Weckner, T. Adams, N. Ghazarian and V. Balabanov, "Large bay skin buckling of composite aircraft structure: method development and validation," in *AIAA SciTech Forum*, Virtual Event, Jan 2021.

[40] T. Hou, J. M. Baughman, T. J. Zimmerman, J. K. Sutter and J. M. Gardner, "Evaluation of sandwich structure bonding in out-of-autoclave processing," in *42nd Int. SAMPE Technical Conf.*, Salt Lake City, UT, 2010.

[41] J. K. Sutter et al., "Comparison of autoclave and out-of-autoclave composites," in *42nd Int. SAMPE Technical Conf.*, Salt Lake City, UT, 2010.

[42] Y. Cai, D. Rajaram and D. N. Mavris, "Multi-mission multi-objective optimization in commercial aircraft conceptual design," in *AIAA Aviation 2019 Forum*, Dallas, TX, Jun 2019.

[43] K. Milios, C. Hall, A. Burrell, J. Brooks, J. Kenny Jr., J. Gladin, D. Mavris, "Modeling and Simulation of a Parallel Hybrid-Electric Propulsion System - Electrified Powertrain Flight Demonstration (EPFD) Program," in *IEEE/ AIAA Transportation Electrification Conf. and Electric Aircraft Tech. Symp.*, Anaheim, CA, 2022.